Taylor & Francis
Taylor & Francis Group

Large-scale interfacial damage and residual stresses in a glass–ceramic matrix composite

Konstantinos G. Dassios* and Theodore E. Matikas

Department of Materials Science and Engineering, University of Ioannina, Ioannina GR-45110, Greece

The current work is concerned with the micro-mechanics of fracture of a SiC-fiber-reinforced barium osumilite (BMAS) ceramic matrix composite tested under both monotonic and cyclic tension. The double-edge notch (DEN) specimen configuration was employed in order to confine material damage within a predefined gage length. The imposition of successive loops of unloading to complete load relaxation and subsequent reloading were found to result in an increase by 20% in material strength as compared to pure tension; the finding is attributed to energy dissipation from large-scale interfacial debonding phenomena that dominated the post-elastic mechanical behavior of the composite. Cyclic loading also helped establish the axial residual stress state of the fibers in the composite, of tensile nature, via a well-defined common intersection point of unloading–reloading cycles. An approach consisting of the application of a translation vector in the stress–strain plane was successfully used to derive the residual stress-free properties of the composite and reconcile the scatter noted in elastic properties of specimens with respect to theoretical expectations.

Keywords: ceramicmatrix composites; interface; residual stresses; mechanical testing

Introduction

First appearing in the 1990s, ceramic matrix composites (CMCs) with continuous reinforcements offer optimized properties compared to monolithic ceramics such as increased fracture toughness, crack growth resistance, damage tolerance and strength, and decreased brittleness. This class of material is less prone to unstable catastrophic failure than the first generations of CMCs due to the damage mechanisms that develop during fracture and consume part of the externally applied energy, decreasing at the same time the energy apportioned to the catastrophic work of crack advance at the crack tip. Continuous-fiber-reinforced CMCs have already replaced ceramics and metals in applications with increased thermo-mechanical performance demands such as aircraft brakes, internal chambers and nozzles of jet motors, thermal barriers, turbine and burner nozzles and space shuttle parts.

The mechanical behavior of CMCs is controlled by the properties of the matrix and fibers, fiber aspect ratio, volume fraction and, most importantly, by the properties of the interface, the fiber-matrix boundary that occupies a vast surface area of the material and is responsible for transferring stresses from the continuous phase to the reinforcements. In composites of heterogeneous constituents, mismatches between the coefficients of thermal expansion (CTE) of the matrix and the fibers occur usually. Under such conditions, during cooling of

---

*Corresponding author. Email: kdassios@cc.uoi.gr

the composite from the manufacturing to room temperature, fibers with a CTE higher than that of the matrix can remain in residual tension; or in residual compression in the inverse scenario. Such internal residual stresses significantly affect the stress transfer characteristics at the interface by inducing micro-cracks in the matrix material. It is then expected that during testing of a composite with constituents of different CTEs, the extent of interfacial damage is directly associated with the thermal residual stress state of the material. Interfacial properties such as the interfacial shear strength also depend on processing conditions. For example, it is known that during hot-pressing of SiC-fiber-reinforced glass–ceramic matrix composites, a chemical reaction between the fiber surface and the oxides in the matrix results in the formation of a carbon-rich interfacial bond [1,2] which is weak enough to result – especially in combination with a brittle matrix – in fiber-bridged matrix cracks when the composite is loaded in tension.

During tensile testing of CMCs with unloading–reloading loops (cyclic tension), a residual-stress-related common intersection point (CIP) of the compliance slopes of the loops may form either experimentally or by extrapolation; it has been shown that the stress coordinate of this point is directly related to the residual stress of fibers in the composite.[3–5] The CIP approach is currently the only plausible method for evaluating therma residual stresses (TRS) from mechanical test data.

The present manuscript reports on the extent of interfacial damage and the residual stress state of a continuous SiC-fiber-reinforced barium osumilite ($BaMg_2Al_6Si_9O_{30}$, BMAS) glass–ceramic matrix composite loaded in cyclic tension. The fiber residual stress was directly evaluated by interrogation of the CIP that was assembled by raw experimental data and the information was used to validate a prevalent theoretical TRS model. The triple-regime tensile behavior associated with interfacial debonding and final material fracture, the effects of negative inelastic strain accumulation, and material damage with respect to the elastic behavior of fibers are discussed in the text.

Experimental

Materials and specimens

Cross-ply SiC/BMAS composite laminates, 3-mm thick, consisted of silicon carbide 'Tyranno' fibers. The nominal elastic modulus and strength of the Tyranno fibers, as quoted by the manufacturer, are 190 and 3.3 GPa, respectively. The composite processing technique consisted of: (1) desizing the Tyranno fiber bundles in a furnace, (2) wetting the desized fibers in a slurry of the precursor glass frit, (3) winding the fibers on a mandrel and allowing to dry for 20 min, (4) cutting and manually arranging the fibers in layers for the preparation of prepreg sheets, (5) stacking the sheets in $(0,90)_{4s}$ sequence, (6) burning the binder off, and (7) hot-pressing in a graphite die at ~1200 °C for 10 min. Final crystallization was achieved by heat treatment at 1300 °C. Fiber volume fraction in the final product was 0.55.

The laminates were cut into rectangular beams of dimensions 100 mm × 12 mm × 3 mm ($l \times w \times t$) in a CNC vertical machining center equipped with a diamond wafering blade. Fiber orientation in the external plies was chosen to result parallel to the loading axis (0°). Notches were prepared using the same equipment. Notch-to-width ratios (notched ligament fractions) of 0.35 and 0.2 were used while un-notched 'dogbone' specimens were prepared for pure tensile loading. Sets of three specimens were prepared for each case. All tensile and cyclic tension tests were carried out in displacement control with a crosshead rate of 0.2 mm/min on a servohydraulic testing frame equipped with a 100 kN load cell and hydraulic clamping grips. A clip-on axial extensometer equipped with knife-edge legs, gage length 25 mm, was used to capture strain. The initial strain rate, calculated for the effective gage

length of 50 mm, was $4.0 \times 10^{-3} \, \text{min}^{-1}$. Unloading to complete relaxation and subsequent reloading cycles commenced at 0.1% strain with a step of 0.15% strain.

Results and discussion

Composite performance under cyclic loading

The typical stress–strain response, under cyclic tension, of three DEN specimens of different notch-to-width ratios of the SiC/BMAS composite is presented in Figure 1. The material's mechanical behavior under monotonic tension is included in the top graph of Figure 1 as a dashed line. It was observed that the stress–strain response of the composite consisted of an initial linear part, followed by a regime of gradually decreasing tangent modulus to the curve. This apparent softening is due to interfacial debonding and slipping between matrix and fiber in the area confined between neighboring matrix blocks interconnected by fiber bundles, formed as a result of matrix cracking in planes perpendicular to the fibers' axis. The average slope of unloading–reloading cycles appeared to decrease with cycle count suggesting a degradation in material stiffness due to progressive matrix and interfacial damage. DEN specimens failed shortly after the attainment of the maximum load; the associated curves exhibited very minimal tail effects.

Un-notched specimens appeared to fail after a final regime of increased apparent stiffness and increased tangent modulus to the curve. Within this regime, large-scale debonding of the interface and matrix cracking are believed to have completed; the load bore by the matrix
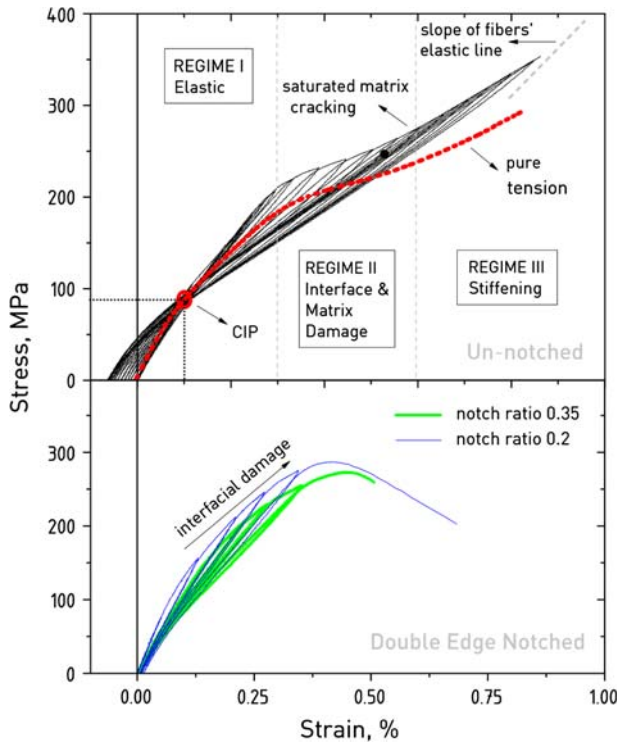

Figure 1. Stress–strain performance of the SiC-fiber-reinforced ceramic matrix composite under cyclic tension.

cannot increase further, and only fibers carry the global load. The prevalent damage mechanism in this regime is hence load bearing by intact fibers, which is superior to the mechanism associated with the interface and the matrix, hence macroscopic stiffening becomes apparent, coupled with an almost linear stress–strain relationship. Catastrophic fracture commences after failure of the first fiber bundle leading to a dramatic decrease in V_f. Other researchers have also reported such stiffening phenomena and linear stress–strain end shapes in composite curves.[6–8]

The stress–strain behavior of specimens without notches was dominated by a uniquely well-defined CIP of unloading–reloading curves that appeared in the first quadrant of the stress–strain curve (tensile domain) at 0.1% strain and 90 MPa stress. Similar CIPs have been previously established by Steen,[3] Camus,[4] and Mei,[5] however, that was done indirectly, by extrapolation of the elastic compliance slopes of each reloading loop and the CIPs fell within the compression domains of their stress–strain curves. Morscher [9] also used the compliance extrapolation method to calculate a tensile residual stress state of SiC-fibers in a SiC matrix. However, a CIP assembling by raw experimental data alone has never been encountered before. CIPs were absent in the tensile curves of notched specimens, as seen in Figure 1. It is believed that machining damage during notch fabrication may have relieved the thermal residual stresses of the composite or the TRS could have relaxed due to the stress concentration introduced by the notches.[10]

Composite elastic modulus appeared to decrease with increasing notch length; average values of 108, 119, and 151 GPa were calculated for specimens with notch-to-width ratios of 0.35, 0.2, and 0. The dependency of modulus on notch length is attributed to the finite dimensions of the gage length compared to the stress concentration region. The classical rule of mixtures expects a modulus of 106 GPa, calculated using a value of $E_m = 120$ GPa [11] for the matrix modulus, a non-unidirectional reinforcement correction factor of $\lambda = 0.5$ accounting only for fibers oriented in the loading direction and a volume fraction of $V_f = 0.55$. As will be shown in the following, the observed difference between the true and theoretically expected moduli is associated with the thermal residual stress state of the composite. Composite strength also appeared to decrease with increasing notch length; average values of 270, 280, and 355 MPa were calculated for specimens with notch-to-width ratios of 0.35, 0.2, and 0.

Indications of large-scale bridging and pull-out throughout the length of the notched ligaments of tested specimens were collected post-mortem: the specimens were received in one free standing piece after removal from the grip with exposed fibers – which had apparently failed within the matrix environment and were pulling-out – still bridging the two sides of the dominant macrocrack, as seen in Figure 2. The mere existence of a pull-out mechanism confirms a weak interfacial bond between the glass matrix and the SiC fibers as expected by chemistry (see section Experimental).

Loop hysteresis, a broadening in the shape of unloading–reloading loops, was evident in all cycles apart from the initial couple that usually fell within the elastic behavior regime of the material. The effect, which also appeared coupled with the introduction of positive curvature on the unloading curves, is believed to be associated with frictional forces developing during sliding of fibers across the matrix along the debonded interface. At small strains, both composite constituents are able to sustain the applied load because the coefficient of friction is still high – hence, no sliding occurs. As strain increases, fiber sliding begins. The maximum width of loops, a parameter that quantifies the magnitude of the hysteresis effect, increased with cycle count within the second-debonding regime and decreased again towards the final cycles in un-notched specimens, as seen in Figure 3. This is because during the last fracture stages, the cracking and debonding mechanisms have reached a saturated state and the applied load is shared only by the intact fiber population.
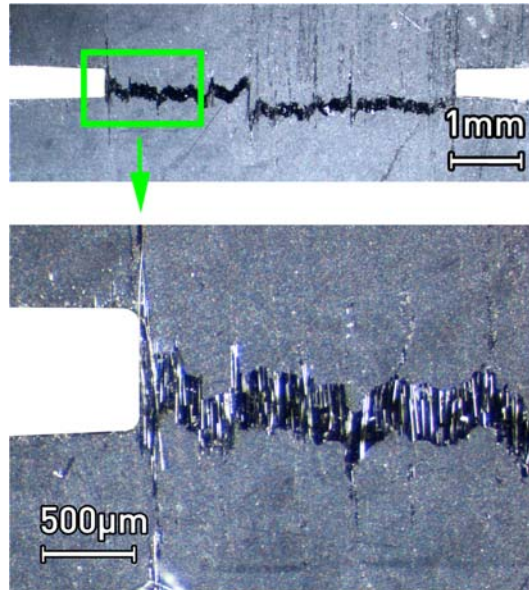
Figure 2. Energy dissipation mechanisms observed in the optical stereoscopy images of notched ligaments of the SiC/BMAS composite: macro- and micro-cracking, crack deflection, large-scale bridging, and pull-out.
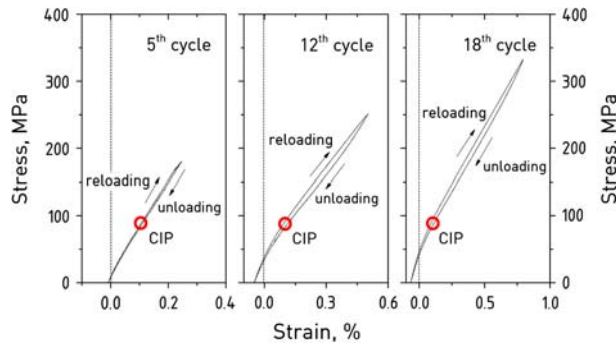

Figure 3. Typical hysteresis shapes of the 5th, 12th, and 18th loops corresponding to the elastic, damage, and stiffening regimes.

The effect of unloading–reloading loops in the mechanical behavior of the un-notched material is an increase by 20% in attainable material stress compared to monotonically tested specimens (Figure 1). Very interestingly, the monotonic tension curve appeared to intersect the cyclic-loading curve exactly at the self-assembled CIP at 0.3% strain. The shapes of the curves were similar for both cyclic and monotonically loaded specimens. For strain values lower than 0.3%, both testing conditions yielded comparable material response. At strains higher than 0.3%, tangent modulus decreased more rapidly in the monotonic tension curve than in the cyclic tension curve. As a consequence, the debond region appeared at lower stresses in monotonic tension than in cyclic tension, still at the same strain of 0.3%. The stiffening regime appeared at strains > 0.6% for both loading conditions. Within this last regime, the tangent modulus decreased more rapidly in monotonic than in cyclic tension curves. Average failure strain values of 0.85% were common for both loading conditions, a finding that suggests that the

effect of cycling on the maximum deformation achievable by the composite is minimal. Based on the above results, it can be concluded that the mechanisms of matrix cracking, large-scale interfacial debonding, and ultimate stiffening are affected by the cyclic loading protocol.

Calculation of the TRS-free origin

Steen has argued that the stress coordinate of CIPs assembled by extrapolation of elastic compliance lines (upper linear part of reloading cycles) is equal to the average axial residual stress in the fibers multiplied by their volume fraction, whereas the strain coordinate corresponds to the axial residual strain in the fibers averaged over the gage length.[3] By application of this argumentation to the experimentally self-assembled CIP of the current work, the axial residual stress and strain of SiC fibers are calculated as 163 MPa and 0.1%, respectively. The tensile nature of residual stresses suggests that longitudinal shrinkage of fibers was restricted by the surrounding matrix during cooling of the material from the firing temperature to ambient temperature. This can only hold if the glass matrix material has a CTE that is lower than the fibers. This is indeed the case as CTEs for BMAS and SiC-Tyranno fibers are around $\alpha_m = 2.5 \times 10^{-6} K^{-1}$ [12] and $\alpha_f = 4.5 \times 10^{-6} K^{-1}$ (according to fiber manufacturer). For a composite with a noncracked matrix and perfect interfacial bonding, a classic theoretical estimation of TRS [5] is given as:

$$\sigma_r^m = E_m \frac{\lambda E_f V_f}{\lambda E_f V_f + E_m V_m}(a_f - a_m)(T_o - T_p) \qquad (1)$$

where, $T_o = 298$ K and $T_p = 1573$ K are the operation and processing temperatures, respectively. Using the already known values of above parameters, the theoretical residual stress is found to be negative at 150 MPa (compressive). Hence, the axial residual stress on the fibers would be tensile at 150 MPa. This value is only 8% less than the experimentally measured TRS. Under the assumption that the CIP is the TRS-free origin of the mechanical behavior of the composite, it would be interesting to examine the effect on properties of translating the whole curve in the stress–strain plane so that the CIP is brought into coincidence with the origin.
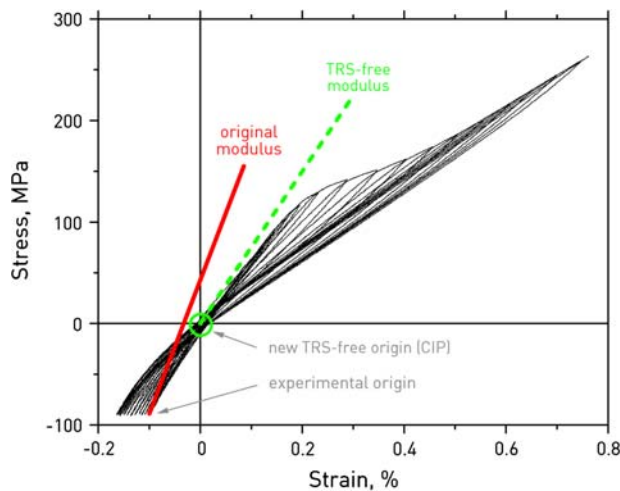

Figure 4. TRS-free mechanical behavior by translation of the stress–strain curve so that the CIP is brought to coincidence with the origin.

This has the effect depicted in Figure 4 and results in a recalculation of the composite elastic modulus at 104 GPa. The new value is by 30% lower than the original modulus and much close to the average modulus of notched specimens, 113 MPa. The above example demonstrates the strong dependence of material properties on residual stress and suggests that quantification of residual stresses is key to reporting accurate and meaningful material properties.

It should not be overlooked that *radial* residual stresses also develop during material processing. These stresses influence the degree of load transfer between the fibers and the matrix across the interface, hence they affect the amount of frictional energy dissipation during interfacial sliding, which is represented by the area of the hysteresis loops during cycling loading. However, this area does not affect the envelope tensile curve and the calculated elastic constants of the material.

Strain offset at relaxation and elastic stiffness

Irrespective of notch presence or not, the curves of all SiC_f/BMAS composites exhibited inelastic strain accumulation upon unloading, calculated as the strain offset at zero load just on the completion of unloading. Inelastic strain is plotted in Figure 5 for specimens of different initial notch lengths as a function of peak cycle stress. It is observed that notched specimens were associated with small values of positive inelastic strains which appeared to increase with notch length. A totally different effect is seen in un-notched specimens: there inelastic strain was negative and reached an absolute maximum value that was 400% higher than the inelastic strain of notched specimens. Negative strain accumulation originates from matrix crack closure occurring when the residual stress in the matrix is compressive (tensile in the fibers) and relief of residual stresses during loading causes an expansion of the matrix blocks and a contraction of fibers bridging the cracks. It was also found that inelastic strain increased with cycle count and attained a plateau value in the final cycles where matrix cracking has completed. The latter observation suggests that inelastic strain is related to the matrix cracking mechanism, most possibly through the mechanical impediment of complete crack closure due to fiber roughness and/or contact between opposing faces micro-crack slightly moved from their original positions during cyclic loading. This explanation is further favored by the increase in tangent modulus of the unloading curves towards the lower ends of the loops.
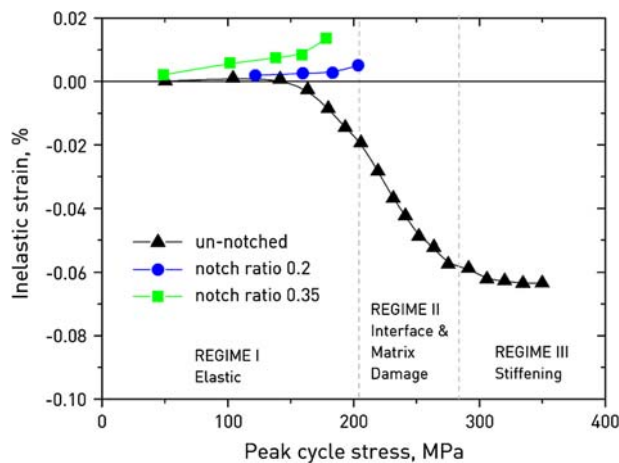

Figure 5.   Inelastic strain plotted for different notch lengths as a function of cycle stress.
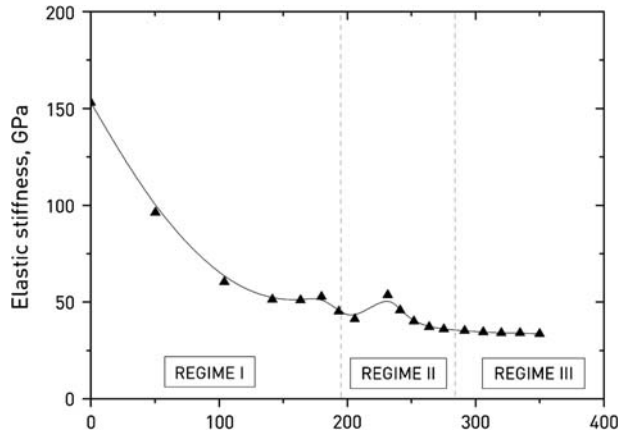
Figure 6.   Elastic stiffness of the SiC/BMAS composite during cyclic loading. The solid line represents a cubic spline regression to the experimental data.

The upper part of the reloading modulus (linear end of reloading curve) is widely accepted as the elastic stiffness, equivalent to the modulus of the damaged material under monotonic tension. By regression to the 17 reloading cycles of Figure 1, the elastic stiffness is plotted as a function of cycle stress in Figure 6. The property appeared to decrease rapidly from the Young's modulus value, 153 GPa, within the initial regime and attain a plateau value of ca. 35 GPa near the end of the damage regime.

Conclusions

Thermal residual stress state was investigated for a continuous SiC-fiber-reinforced BMAS-ceramic matrix composite tested under tension with unloading–reloading cycles. The stress–strain response of un-notched composites exhibited a triple regime consisting of an initial elastic regime, a subsequent softening regime due to large-scale interfacial debonding, and a final regime of apparent stiffening and increase in modulus due to load bearing by intact fibers in a completely cracked matrix. The latter regime was not evident in notched specimens of the same material. The coordinates of the CIP of unloading–reloading cycles in the tensile curves of un-notched specimens were used to directly measure the thermal residual stress state of reinforcing fibers as 163 MPa. The introduction of cyclic loading resulted in material strengthening with respect to pure tension; the envelope of the cyclic tension curves appearing at stresses up to 20% higher than that achieved by specimens tested in monotonic tension. The evolution of inelastic strain accumulation and of elastic stiffness was quantified and discussed in the text.

References

[1] Cooper RF, Chyung K. Structure and chemistry of fiber matrix interfaces in silicon-carbide fiber-reinforced glass ceramic composites – an electron-microscopy study. J. Mater. Sci. 1987;22:3148–3160.
[2] Benson PM, Spear KE, Pantano GC. Interfacial characterisation of glass matrix/Nicalon SiC fiber composites: a thermodynamic approach. Ceram. Eng. Sci. Proc. 1988;9:663–670.
[3] Steen M. Tensile mastercurve of ceramic matrix composites: significance and implications for modelling. Mat. Sci. Eng. A-Struct. 1998;250:241–248.
[4] Camus G, Guillaumat L, Baste S. Development of damage in a 2D woven C/SiC composite under mechanical loading.1. Mechanical characterization. Compos. Sci. Technol. 1996;56:1363–1372.

[5] Mei H. Measurement and calculation of thermal residual stress in fiber reinforced ceramic matrix composites. Compos. Sci. Technol. 2008;68:3285–3292.

[6] Wang M, Laird C. Characterization of microstructure and tensile behavior of a cross-woven C-SiC composite. Acta Mater. 1996;44:1371–1387.

[7] Wang MD, Laird C. Tension-tension fatigue of a cross-woven C/SiC composite. Mater. Sci. Eng. A-Struct. 1997;230:171–182.

[8] Cady C, Heredia FE, Evans AG. Inplane mechanical-properties of several ceramic–matrix composites. J. Am. Ceram. Soc. 1995;78:2065–2078.

[9] Morscher GN, Singh M, Kiser JD, Freedman M, Bhatt R. Modeling stress-dependent matrix cracking and stress-strain behavior in 2D woven SiC fiber reinforced CVISiC composites. Compos. Sci. Technol. 2007;67:1009–1017.

[10] Johnsonwalls D, Evans AG, Marshall DB, James MR. Residual-stresses in machined ceramic surfaces. J. Am. Ceram. Soc. 1986;69:44–47.

[11] Widjaja S. Determination of creep-induced residual stress in fiber-reinforced glass–ceramic matrix composites by X-ray diffraction. Mater. Charact. 2001;47:47–54.

[12] Jais US, Lee WE, James PF. Crystallization of barium osumilite glass. J. Am. Ceram. Soc. 1999;82:3200–3208.